RSC Advances

PAPER

View Article Online
View Journal | View Issue

Check for updates

Cite this: *RSC Adv.*, 2022, **12**, 23427

UiO-66-NH_2 based fluorescent sensing for detection of tetracyclines in milk†

Xiaohui Wang * and Xufeng Wang

Received 29th June 2022
Accepted 5th August 2022

DOI: 10.1039/d2ra04023a

rsc.li/rsc-advances

In this work, a fluorescent sensor based on a zirconium-based metal organic framework was prepared for the detection of tetracyclines (TCs) in milk. The UiO-66-NH_2 fluorescent sensor was synthesized by a simple microwave-assisted method with 2-aminoterephthalic acid and zirconium chloride as precursors. In the presence of target TCs, the synergistic effect of the inner filter effect (IFE) and photo-induced electron transfer (PET) was responsible for the fluorescence quenching of UiO-66-NH_2, and the fluorescence sensor showed a rapid fluorescence quenching response (5 min) to target TCs. The proposed UiO-66-NH_2 sensor had good sensitivity and selectivity, and under the optimal conditions possessed detection limits of 0.449, 0.431, and 0.163 μM for tetracycline (TET), oxytetracycline (OTC), and doxycycline (DOX), respectively. Besides, the UiO-66-NH_2 sensor was successfully applied to the quantitative detection of TCs in milk samples with reasonable recoveries of 93.26–115.17%, and the detection results achieved from the as-fabricated fluorescence sensing assay were consistent with those of high-performance liquid chromatography (HPLC), indicating the potential applicability of the UiO-66-NH_2 sensor for detecting TCs in actual food samples.

1. Introduction

As common broad-spectrum antibacterial agents, tetracyclines (TCs), including tetracycline (TET), oxytetracycline (OTC), and doxycycline (DOX), are extensively used in both humans and animals to prevent and treat bacterial infections caused by both Gram-positive and Gram-negative bacteria because of the favourable antibacterial effect, minor side effects, good absorption, and relative low cost.[1–3] In addition, TCs are also employed as feed additives in animal husbandry to promote growth and enhance the feed-to-weight ratio.[4–6] However, the rampant use of TCs in veterinary medicine may result in their residues in animal origin food, such as milk,[7] meat,[8,9] and eggs,[10] which would be a threat to human health.[11–14] Moreover, consumption of foodstuffs containing TC residues for long periods will lead to the spread of resistant bacteria strains through the food chain and cause other adverse reactions, such as allergic syndromes, kidney damage, and hepatotoxicity.[15–19] In order to reduce the negative effects of TCs and protect the health of consumers, the Commission Regulation (EU) no. 37/2010 has set a maximum residue limit (MRL) of 100 ppb for TCs in milk matrix.[16,20] And, the MRL for TCs in milk defined by the Food and Drug Administration (FDA) in US is 676 nM (300 ng mL^{-1}).[7]

To date, the methods of TCs detection in food industry mainly include high performance liquid chromatography (HPLC),[14,21–23] liquid chromatography-tandem mass spectrometry (LC-MS/MS),[24] capillary electrophoresis (CEP),[25,26] enzyme-linked immunoassay (ELISA),[27–29] microbiological method,[30,31] and electrochemistry analysis.[32,33] However, these analytical approaches always have some defects in detection, such as long detection time, complex sample pre-processing procedure, expensive experimental instrument, trained professional technology, low sensitivity and specificity, or poor reproducibility of experimental results, limiting their practical application in dairy products.[34] Among them, HPLC is the most commonly used method with good selectivity and sensitivity, but often requires cumbersome sample preparation. ELISA has the advantages of simple pre-treatment and low cost, but it always takes time and usually suffers from low sensitivity and even the possibility of false positive results. Although CEP has short analysis time and easy operation, it inevitably still has the problems of poor reusability and low sensitivity. Microbiological assay is facile and the cost is the lowest, but it subjects to its inferior specificity and sensitivity. Despite of the outstanding sensitivity and selectivity, electrochemical analysis is difficult to be applied for the repeated detection of trace TCs. Consequently, the development of simple, rapid, sensitive, and reliable methods for the determination of TCs residues in milk is of great significance.

In recent years, fluorescent sensing method has been exploited and utilized in the detection of TCs owing to its advantages of easy operation, low-cost, fast response and high

State Key Laboratory of Food Nutrition and Safety, Tianjin University of Science and Technology, Tianjin 300457, China. E-mail: xhw2022tjin@163.com

† Electronic supplementary information (ESI) available. See https://doi.org/10.1039/d2ra04023a

Open Access Article. Published on 17 August 2022. Downloaded on 7/15/2025 3:50:19 PM. This article is licensed under a Creative Commons Attribution-NonCommercial 3.0 Unported Licence.

Open Access Article. Published on 17 August 2022. Downloaded on 7/15/2025 3:50:19 PM. This article is licensed under a Creative Commons Attribution-NonCommercial 3.0 Unported Licence.

sensitivity.[35] According to different fluorescent materials, such as organic dyes,[36] quantum dots (QDs),[37] metal nanoparticles (MNPs),[38] carbon dots (CDs),[39] upconversion nanoparticles (UCNPs),[40] silicon nanodots (SiNDs),[41] and molybdenum disulfide nanoplates (MoS_2 NPs),[42] a series of fluorescent sensors for TCs detection have been established. Nevertheless, the wide application of above-mentioned materials may be affected by their inherent deficiencies. Organic dyes usually suffer from hindrances of short fluorescence time, low solubility and poor stability. Conventional QDs have the disadvantages of complex and harsh synthesis process, high toxicity and bad biocompatibility. MNPs (especially precious metal nanoparticles) possess the drawbacks of low stability and high cost. SiNDs have intrinsic advantages, *e.g.*, great stability, minimal toxicity, and favourable biocompatibility, but when it comes to photoluminescence (PL) efficiency, they still fall behind the direct band-gap-based QDs. For MoS_2 NPs, the preparation of high quantum yield and well water-soluble fluorescent MoS_2 materials is still a challenge. The tedious operation procedures and low product yield limit the application of UCNPs. In contrast, CDs have the merits of low cost and cytotoxicity, good biocompatibility and high photo stability, but they are too small to separate and purify. As a result, the further improvements are required before these materials can be extensively used in actual samples.

Compared with other fluorescent materials, fluorescent metal–organic frameworks (FMOFs) is a new fast-developing type of crystalline materials, which have the virtues of simple synthesis, permanent porosity, adjustability, and structural diversity of metal organic frameworks (MOFs).[43,44] In addition, FMOFs can also generate fluorescent signals visible to the naked eye, and the development of fluorescence spectroscopy is quite mature.[45] Therefore, FMOFs have a wide range of applications in various targets sensors, *e.g.*, explosive sensors, gas sensors, biomolecule sensors, humidity sensors, temperature sensors, volatile organic compounds (VOC) sensors, and ion sensors.[44] At present, multiple synthetic techniques, including conventional solution reaction, solvothermal method, diffusion method and post-synthetic modification (PSM) strategy, have been developed and utilized for the synthesis of MOFs.[46,47] Of these, conventional solution reaction is simple and fast, but the synthesized MOF compounds are often unstable. Although large size single crystals can be obtained by diffusion method, the low yield and long reaction time limit the widespread application of this method. PSM enables the MOF to have better functional groups and active sites in order to achieve excellent functional properties, but the post modification reaction of MOF often requires the participation of liquid or solution, and this reaction process is difficult to monitor. Compared with other methods, solvothermal method is conducive to the single crystal growth of MOF products, which is the main reason why solvothermal method is widely used. For all that, it usually takes a long reaction time (half a day to several days). It is worth noting that this deficiency can be improved by solvothermal synthesis with microwave-assisted heating method.[48,49] Considering the virtues of short synthesis time, energy saving, high yield and relatively uniform crystal size, microwave-assisted synthesis assay is expected to become a common synthesis method of MOFs.[48]

Up to now, the reported luminescent forms of FMOFs are mainly summarized as follows: (i) organic ligand-based luminescence; (ii) lanthanide ions luminescence; (iii) charge-transfer luminescence; and (iv) guest-induced luminescence, which offers a strong theoretical basis for fluorescence sensing.[46] Even so, owing to the reversibility of coordinate bonds, the stability of FMOFs, especially water stability, is still a problem to be solved.[44] With the foundation of hard/soft acid/base (HSAB) theory, stable MOF can be composed of tetravalent metal ion Zr^{4+} and carboxylate-based ligands.[50] Among various metal organic frameworks, zirconium (Zr)-based MOFs have good development prospects in fluorescence sensing due to their excellent stability, structural diversity, and fascinating characteristics.[51] Besides, the stability of FMOFs and the sensitivity of the detection system will be well improved by introducing functional groups (such as amino groups).[47,52–54] It has been reported that the amino groups introduced in the materials can combine with TCs by hydrogen bonding interaction, leading to fluorescence quenching through electron transfer between the analyte molecule and the fluorescence sensor.[7] UiO-66-NH_2, one of the Zr-based MOFs, has been used for the fluorescence detection of fluoride ion and the adsorption of mercury in aqueous solution because of its highly stability in water and even in mild acid-base environment.[55–57] Therefore, amino functionalized Zr-MOF (UiO-66-NH_2) was selected to detect TCs in milk in this research considering its stability toward water and organic solvents. Simultaneously, microwave-assisted synthesis method was chosen to synthesize the UiO-66-NH_2 in this work. As far as we know, there has been no report on detection of TCs in milk based on UiO-66-NH_2 fluorescence sensor.

In this paper, we used a facile microwave-assisted synthesis method to prepare UiO-66-NH_2 fluorescent sensor for detecting TCs residues in milk. The UiO-66-NH_2, synthesized through utilizing Zr^{4+} as metal centre and 2-aminoterephthalic acid (ATA) as organic linker, contained abundant $-NH_2$ on its surface, which increased its stability in water and provided a binding site for target TCs (Fig. 1). The as-prepared UiO-66-NH_2 possessed good fluorescence performance, and could be quenched by TCs because of photo-induced electron transfer (PET) (the electron transfer from ATA organic ligand to TCs) and inner filter effect (IFE). Moreover, the hydrogen bond interaction between amino groups on UiO-66-NH_2 and hydroxyl groups of TCs enabled the fluorescence sensor to detect TCs specifically from a series of interference factors (antibiotics, ions and amino acids). Eventually, due to high sensitivity and excellent selectivity, the established fluorescence sensing analysis method was successfully applied to detect TCs in actual milk samples with desirable results.

2. Experimental section

2.1. Reagents and materials

Zirconium chloride ($ZrCl_4$, 98%) was obtained from Beijing Yinuokai Technology Co., Ltd (Beijing, China). *N*,*N*-

 © 2022 The Author(s). Published by the Royal Society of Chemistry

Open Access Article. Published on 17 August 2022. Downloaded on 7/15/2025 3:50:19 PM.
This article is licensed under a Creative Commons Attribution-NonCommercial 3.0 Unported Licence.

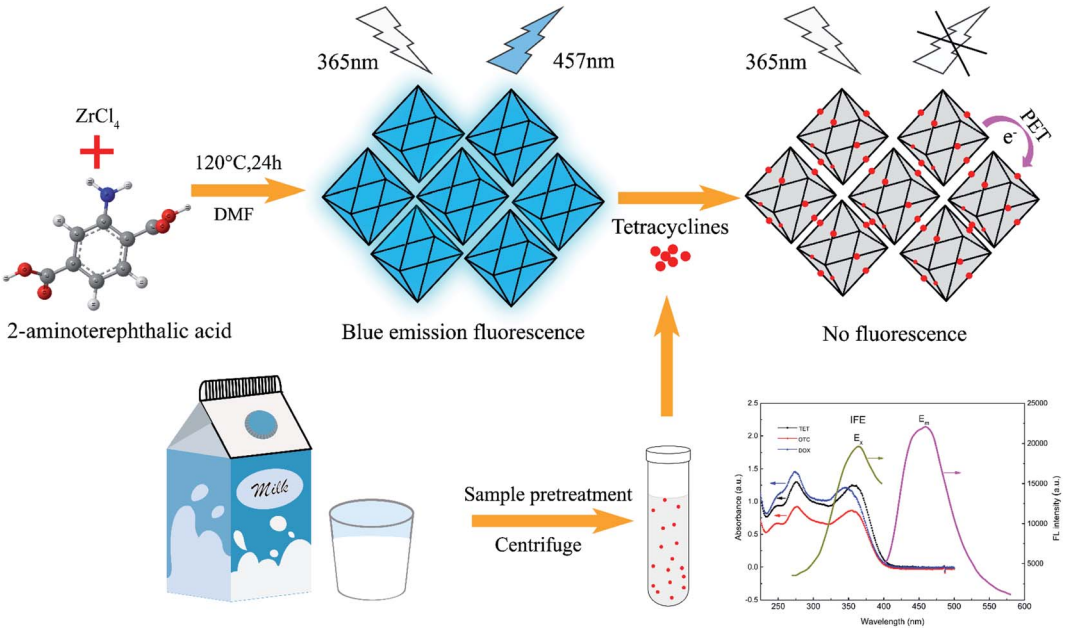

Fig. 1 Establishment of UiO-66-NH_2 fluorescence sensing system for TCs detection in milk.

Dimethylformamide (DMF), ethyl alcohol (EtOH), $Zn(NO_3)_2 \cdot 6H_2O$, $AlCl_3 \cdot 6H_2O$, $MgCl_2 \cdot 6H_2O$, $MnCl_2 \cdot 4H_2O$, KCl, $CaCl_2$, and NaCl were from SinopharmChemical Reagent Co., Ltd (Shanghai, China). 2-Aminoterephthalic acid (ATA, 98%), tetracycline (TET), doxycycline (DOX), oxytetracycline (OTC), ampicillin (AMP), amoxicillin (AMX), chloramphenicol (CM), cysteine (Cys), tyrosine (Tyr), phenylalanine (Phe), serine (Ser), arginine (Arg), and histidine (His) were purchased from Shanghai Macklin Biochemical Co., Ltd (Shanghai, China), and the chemical structural formulas of TCs were displayed in Fig. S1.† All chemical reagents used were of analytical grade and did not require further purification. During the entire study, doubly deionized water (DDW, 18.2 MΩ cm^{-1}) obtained by a Milli-Q water purification system was used. The fresh milk sample applied in the experiment was purchased from a local supermarket.

2.2. Instruments

The morphology of UiO-66-NH_2 was observed by the scanning electron microscopy (SEM, Hitachi, Japan) and transmission electron microscope (TEM, JEOL, Japan). The Fourier transform infrared spectroscopy (FT-IR) spectra were acquired using a Tensor-37 FT-IR spectrophotometer (Bruker, Germany), and the X-ray photoelectron spectroscopy (XPS) was carried out by an Axis Ultra DLD X-ray photoelectron spectrometer (Kratos, England). UV-vis absorption spectra were obtained by an ultraviolet spectrophotometer (Victoria, Australia), and the fluorescence spectra were recorded on a Lumina fluorescence spectrophotometer (Thermo, USA). The results obtained from the UiO-66-NH_2 sensor was validated by HPLC (LC-20AB, Shimadzu, Japan).

2.3. Synthesis of UiO-66-NH_2

UiO-66-NH_2 was prepared according to the previous study with a little modification.[57] First, 669 mg (2.87 mmol) of $ZrCl_4$ and 500 mg (2.76 mmol) of 2-aminoterephthalic acid (ATA) were dissolved in 60 mL of DMF. Next, the mixture solutions were ultra-sonicated for 30 min at room temperature. Then, the mixture was transferred to a 100 mL stainless steel Teflon-lined autoclave and heated at 120 °C for 24 h in an oven. After being cooled to room temperature, the resulting solid was collected by centrifugation and then dispersed in 24 mL of absolute ethyl alcohol. Subsequently, the dispersion was transferred to a microwave-assisted heating device and maintained at 100 °C for 30 min. Finally, the resulting solid product was centrifuged and dried in a vacuum-drying oven at 70 °C overnight.

2.4. Fluorescence sensing experiment of TCs

The typical experimental procedure for fluorescence detection of TCs was as follows. Firstly, the stock solutions of TET, OTC and DOX were separately prepared, and diluted to the required concentrations before the experiment. Secondly, TCs standard solutions with various concentrations were respectively mixed with 0.1 mg mL^{-1} UiO-66-NH_2 solution (v/v, 1 : 1) at ambient temperature in a centrifuge tube, with the final TET concentrations of 1.25, 5, 7.5, 10, 12.5, 15, 17.5, 20, 27.5, 35, 37.5, 40, 47.5 μM, DOX concentrations of 0.25, 2.5, 5, 7.5, 10, 12.5, 15, 17.5, 20, 27.5, 30, 32.5, 37.5, 40 μM, and OTC concentrations of 0.25, 2.5, 5, 7.5, 10, 12.5, 15, 17.5, 20, 27.5, 30, 37.5 μM, and the concentration of UiO-66-NH_2 in the mixture was 0.05 mg mL^{-1}. Sequentially, the above reaction systems (pH = 8) were incubated at room temperature for 5 min in the dark, and the fluorescence spectra from 400 to 520 nm under the excitation at 365 nm were recorded. Furthermore, the mixture of UiO-66-NH_2

© 2022 The Author(s). Published by the Royal Society of Chemistry

Open Access Article. Published on 17 August 2022. Downloaded on 7/15/2025 3:50:19 PM.
This article is licensed under a Creative Commons Attribution-NonCommercial 3.0 Unported Licence.

solution and deionized water (v/v, 1 : 1) was set as the control group. All the fluorescence experiments were performed in parallel three times.

2.5. Selectivity for TCs

To study the selectivity of the proposed fluorescence method for the detection of TCs, the following selective experiments were carried out. Several possible interferences (AMP, AMX, CM, Cys, Tyr, Phe, Ser, Arg, His, Al^{3+}, Mg^{2+}, Mn^{2+}, Ca^{2+}, Zn^{2+}, Na^{+}, and K^{+}) were added to UiO-66-NH_2 solution respectively in the presence of TCs (50 μM). After incubation for 5 min at ambient temperature, the fluorescence intensity of each mixed system was measured.

2.6. Detection of TCs in milk

Milk samples bought from local supermarket were selected for actual sample analysis to verify the feasibility of the established fluorescence sensing method. According to the pre-treatment procedure in the previous work,[18,58,59] in brief, 1% (v/v) trichloroacetic acid (10%, w/v) and chloroform were first added to the milk sample (5 mL), and vortically mixed for 2 min to precipitate proteins and dissolve other organic substances in the milk matrix. Secondly, the mixture was centrifuged at 11 000 rpm for 15 min to remove the deposit after being sonicated for 15 min. Finally, the supernatant was filtered through a 0.22 μM microporous membrane to remove the lipids, and the filtrate was diluted to a final volume of 10 mL for further analysis according to the procedure in section 2.4. In the recovery experiment, the spiked samples containing standard TCs solutions of 0, 5, 20, and 40 μM were achieved by the standard addition method, and then the pre-processing was carried out according to the above steps.

2.7. Validation by HPLC

Additionally, to validate the reliability of the fluorescence analysis results, traditional HPLC was also used to detect TCs in spiked samples. The HPLC experiment could be successfully completed using oxalic acid (0.01 M)/acetonitrile/methanol (77/18/5, v/v/v) as the mobile phase with a flow-rate of 1.0 mL min^{-1} at 40 °C through a Thermo Scientific-C18 analytical column (4.6 mm × 250 mm, 5 μm). The ultraviolet detector wavelength was set at 350 nm, and the injection volume of each sample was 20 μL.

3. Results and discussion

3.1. Characterization

SEM and TEM were performed to present the surface morphology of UiO-66-NH_2. Fig. 2 showed that the as-prepared UiO-66-NH_2 had nearly octahedron-like appearance with the average edge length of approximately 100 nm.[60,61] FT-IR spectra of UiO-66-NH_2 and ligand 2-aminoterephthalic acid were exhibited in Fig. 3a. In the high frequency region, the characteristic peaks at 3373 cm^{-1} and 3492 cm^{-1} were assigned to the symmetric and asymmetric stretching bands of N–H bonding in amine moieties, respectively.[7,57,62,63] Compared with FT-IR

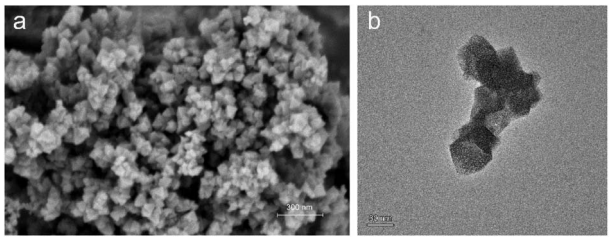

Fig. 2 SEM (a) and TEM (b) images of UiO-66-NH_2.

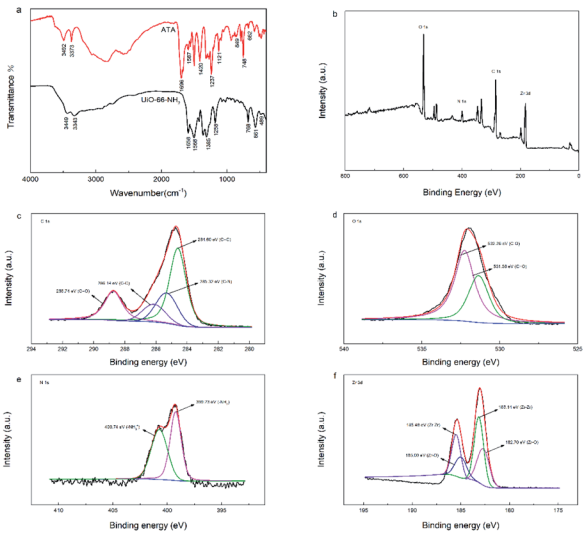

Fig. 3 FT-IR spectra of ATA, and UiO-66-NH_2 (a), and XPS spectra of survey (b), C 1s (c), O 1s (d), N 1s (e) and Zr 3d (f) for the UiO-66-NH_2.

spectrum of ATA, after the introduction of tetravalent zirconium ions, the aforementioned characteristic doublet of stretching vibration in UiO-66-NH_2 shifted to lower wavenumber, indicating that the distribution of amines in MOF was unordered.[57,64] Clearly, the wide absorption band in the region of 2500–3300 cm^{-1} (–COOH) disappeared, signifying that the ATA connected to the UiO-66-NH_2 framework was completely deprotonated.[53,65] In the lower frequency region, the unique C–N stretching absorption in aromatic amines was observed at 1258 cm^{-1}. In addition, the –OCO stretching peaks were obtained at 1658 and 1385 cm^{-1}, proving the formation of dehydroxylation phase in UiO-66-NH_2 after the coordination between ATA and Zr^{4+}.[57,62] The peaks at 768, 661, and 489 cm^{-1} corresponded to the bending vibration of O–H and C–H mixing with Zr–O bond.[56] The above characterization results indicated that UiO-66-NH_2 was successfully achieved.

The element compositions and surface chemical states of UiO-66-NH_2 were analysed using XPS (Fig. 3b–f). As shown in Fig. 3b, peaks corresponding to O 1s, C 1s, N 1s, and Zr 3d were obviously identified in survey spectrum, indicating that UiO-66-NH_2 was primarily composed of C, O, N and Zr. Fig. 3c illustrated the C 1s spectrum could be decomposed into four peaks, owing to the C=C (284.60 eV), C–N (285.32 eV), C–C (286.14 eV) and C=O bonds (288.74 eV) in UiO-66-NH_2, respectively.[60,66] For

© 2022 The Author(s). Published by the Royal Society of Chemistry

Open Access Article. Published on 17 August 2022. Downloaded on 7/15/2025 3:50:19 PM.
This article is licensed under a Creative Commons Attribution-NonCommercial 3.0 Unported Licence.

the O 1s spectrum (Fig. 3d), peaks with binding energy of 531.36 eV and 532.26 eV were attributed to C=O and C–O bonds, respectively.[61,67] As presented in Fig. 3e, the peaks located at 399.23 eV and 400.73 eV in N 1s spectrum were respectively assigned to amino groups (–NH_2) and protonated amine (–NH^{3+}) groups.[60,61] In Fig. 3f, the Zr 3d peak could be further divided into four peaks. The characteristic peaks at 182.70 eV and 185.00 eV corresponded to the Zr–O bonds, and the specific peaks at 183.14 eV and 185.48 eV belonged to the Zr–Zr bonds.[60,66–68]

3.2. Fluorescence (FL) stability of UiO-66-NH_2

The fluorescence emission spectra of UiO-66-NH_2 under different excitation wavelengths (310–400 nm) were recorded in Fig. 4a. At different excitation wavelengths, the maximum emission intensities were displayed at 457 nm, showing good excitation independence. The emission peak at 457 nm of UiO-66-NH_2 under the optimal excitation wavelength of 365 nm was independent of the excitation wavelength, which might reduce the interference of automatic fluorescence in the detection process.

Moreover, the fluorescence response of UiO-66-NH_2-aqueous solution during room temperature storage was repeatedly detected. As presented in Fig. 4b, there was no remarkable fluorescence change within 15 days, indicating that the synthesized UiO-66-NH_2 had desirable photo stability. In addition, UiO-66-NH_2 showed good fluorescence stability in the pH range from 6.0 to 10.0 with negligible fluorescence change (Fig. S2†).

3.3. Optimization of experimental parameters

In order to improve the analytical performance of the UiO-66-NH_2 fluorescence sensor system, a series of experimental parameters (the concentration of UiO-66-NH_2, the temperature and pH of the reaction system, and the incubation time) were optimized.

3.3.1 Incubation time. As the incubation time increased from 0 to 5 min, the fluorescence intensity of UiO-66-NH_2 decreased rapidly, and then reached an equilibrium (Fig. 5a), proving that the reaction between TCs and UiO-66-NH_2 was completed rapidly within 5 min. Therefore, 5 min was selected as the optimal incubation time for subsequent experiments.

3.3.2 UiO-66-NH_2 concentration. The effect of UiO-66-NH_2 concentration in the system was studied by the quenching

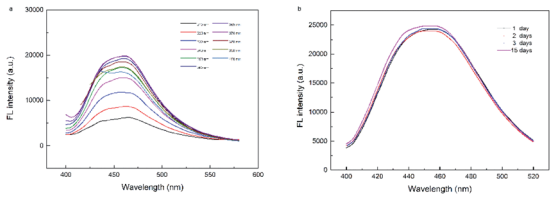

Fig. 4 (a) Fluorescence emission spectra of UiO-66-NH_2 at different excitation wavelengths. (b) Fluorescence (FL) stability of UiO-66-NH_2 for 15 days in room temperature.

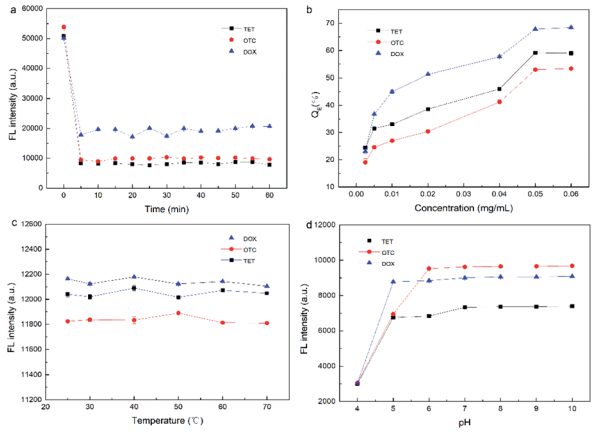

Fig. 5 The effects of incubation time (a), reaction temperature (c) and pH (d) on the fluorescence intensity of UiO-66-NH_2 after introducing TCs. (b) The fluorescence quenching efficiency (Q_E (%)) of TCs in the presence of different concentrations of UiO-66-NH_2.

efficiency of TCs (Q_E (%)). The calculation formula of quenching efficiency (Q_E (%)) can be determined by the eqn (1):

$$Q_E(\%) = \frac{(F_0 - F)}{F} \times 100\% \quad (1)$$

where F_0 and F are the fluorescence intensities of UiO-66-NH_2 in the absence and presence of TCs (0.05 mg mL^{-1}), respectively. The results shown in Fig. 5b demonstrated that Q_E (%) increased significantly with the concentration of UiO-66-NH_2 changing from 0.0025 to 0.05 mg mL^{-1}, and then reached a stable level after the concentration was more than 0.05 mg mL^{-1}, which might be attributed to the sufficient reaction between TCs and UiO-66-NH_2. Consequently, the optimized concentration of UiO-66-NH_2 in the reaction system was 0.05 mg mL^{-1}.

3.3.3 Temperature of reaction system. As shown in Fig. 5c, after the introduction of TCs, the fluorescence response of UiO-66-NH_2 in the reaction system hardly changed at the actual incubation temperature of 25–70 °C, illustrating that the temperature had no significant impact on the detection of TCs. Accordingly, room temperature was used as the reaction temperature of the fluorescence system in this research.

3.3.4 pH of reaction system. The FL intensity of UiO-66-NH_2 at different pH after introducing TCs was studied. As presented in Fig. 5d, in the pH range from 4.0 to 6.0, the FL intensity of UiO-66-NH_2 increased dramatically, while the FL intensity changed slightly in the pH range of 6.0–10.0. Hence, pH 8.0 was chosen for further experiments.

In summary, the UiO-66-NH_2 concentration of 0.05 mg mL^{-1}, incubation time of 5 min, room temperature and pH of 8.0 were adopted as the optimal experimental conditions.

3.4. Fluorescence detection of TCs and calibration curve

The fluorescence response of UiO-66-NH_2 sensor system to different concentrations of TCs was explored in detail. According to the obtained spectra (Fig. 6), it was found that the fluorescence intensity of UiO-66-NH_2 gradually declined with the

Open Access Article. Published on 17 August 2022. Downloaded on 7/15/2025 3:50:19 PM.
This article is licensed under a Creative Commons Attribution-NonCommercial 3.0 Unported Licence.

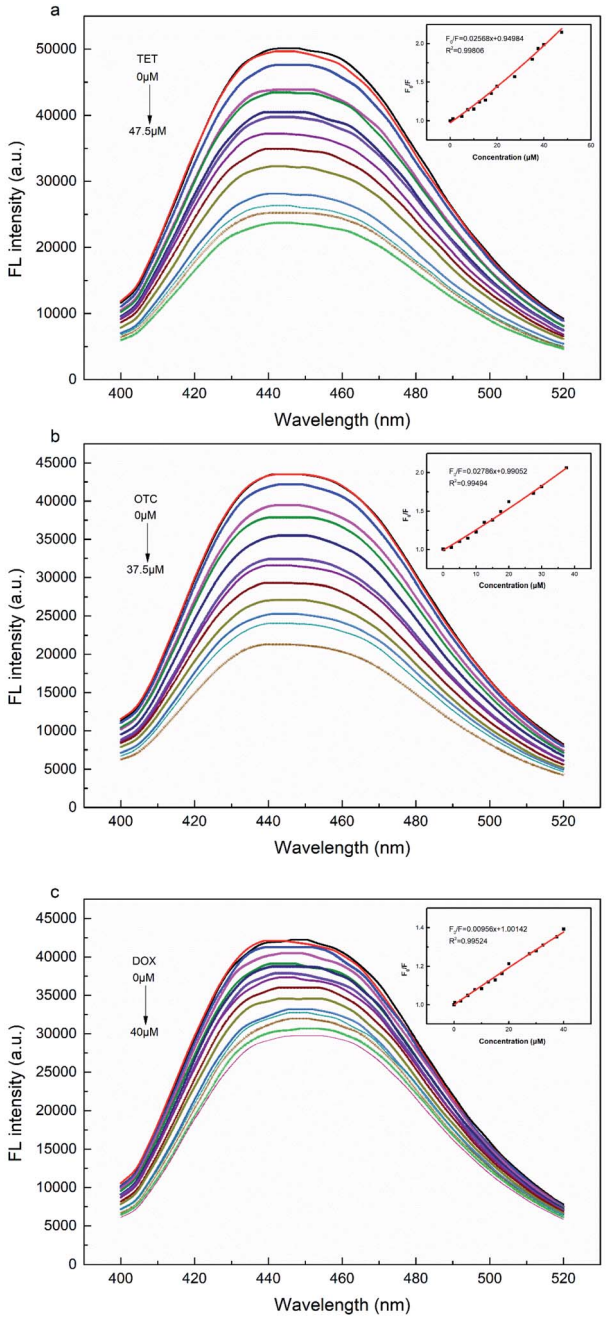

Fig. 6 Fluorescence emission spectra of UiO-66-NH_2 with different concentrations of (a) TET, (b) OTC, and (c) DOX (excited at 365 nm); insets: Stern–Volmer plots for the fluorescence quenching factor F_0/F upon addition of various concentrations.

increase of TCs concentration from 0 to 50 μM, indicating that the established fluorescence sensor system has a high sensitivity. Fluorescence quenching could be described by Stern–Volmer eqn (2):

$$\frac{F_0}{F} = 1 + K_{SV}C_q \quad (2)$$

where F_0 and F are the fluorescence intensities of UiO-66-NH_2 without and after adding TCs, respectively. K_{SV} is the quenching constant (M^{-1}), and C_q is the concentration of TCs. The Stern–Volmer graphs in Fig. 6 (insets) showed that F_0/F of UiO-66-NH_2 increased with a linear relationship to the concentrations of TCs, and the ranges of linearity were 0–37.5 μM for OTC, 0–47.5 μM for TET, 0–40 μM for DOX. Moreover, the K_{SV} were 0.028 (OTC), 0.026 (TET) and 0.010 μM^{-1} (DOX), obtained by the slopes of the regression equations. The limit of detection (LOD) was evaluated by the eqn (3):

$$LOD = 3\frac{S_b}{K_{SV}} \quad (3)$$

where S_b is the standard deviation of eleven blank measurements and K_{SV} is the slope of the calibration curve. Therefore, the LOD values were 449.30 nM for TET, 430.83 nM for OTC, and 163.49 nM for DOX, respectively, lower than the maximum residue limit of 676 nM (300 ng mL^{-1}) for TCs in milk defined by the Food and Drug Administration (FDA) in US. Meanwhile, the LOD (163.49 nM) of DOX was also below the allowed concentrations specified by European Union (EU) for TCs in milk of 225 nM (100 ng mL^{-1}).

3.5. Possible fluorescence sensing mechanism

In general, the fluorescence quenching mechanisms between analytes and sensors were mainly related to three processes: inner filter effect (IFE), fluorescence resonance energy transfer (FRET), and photo-induced electron transfer (PET).[7,36,69,70] Considering that there was almost no effective overlap between the UV absorption band of TCs and the emission band of UiO-66-NH_2 (Fig. 7a), the FRET mechanism was excluded.[71,72] However, noticeably, the excitation spectrum of UiO-66-NH_2 partially overlapped with UV-vis absorption spectra of TCs (Fig. 7a), which manifested the possibility of IFE. As previously reported, the fluorescence lifetime of the fluorophore remains unchanged if IFE occurs, while it reduces as the result of energy transfer during FRET process.[72–74] Accordingly, we took the fluorescence lifetime as an important index to further explain the quenching mechanism and the decay curves of UiO-66-NH_2 and UiO-66-NH_2 + TCs were portrayed in Fig. S3.† There was no significant change in the fluorescence lifetime of UiO-66-NH_2 before and after the addition of TCs, which further verified that the fluorescence quenching mechanism induced by TCs was IFE rather than FRET. The strong absorption of TCs effectively suppressed the excitation energy absorption of UiO-66-NH_2 at the excitation wavelength of 370 nm, resulting in low populated emissive state of UiO-66-NH_2, and the fluorescence of UiO-66-NH_2 was significantly quenched after the addition of target TCs.[7,70] Moreover, the FT-IR spectra of UiO-66-NH_2 + TCs were also displayed in Fig. 7b. After introduction of TCs, the characteristic peaks of $-NH_2$ at 3373 cm^{-1} and 3470 cm^{-1} weakened, and a new wide absorption peak of O–H appeared at 3420 cm^{-1}, showing the hydrogen bond interaction between the amino group on the surface of UiO-66-NH_2 and the hydroxyl group on TCs.[7,65] In addition, the weakening of –C=O stretching absorption at 1660 cm^{-1}, the formation of a new absorption peak at 1619 cm^{-1}, and the red shift of the UV absorption spectrum of the UiO-66-NH_2 after the addition of TCs (Fig. 7c)

© 2022 The Author(s). Published by the Royal Society of Chemistry

Open Access Article. Published on 17 August 2022. Downloaded on 7/15/2025 3:50:19 PM.
This article is licensed under a Creative Commons Attribution-NonCommercial 3.0 Unported Licence.

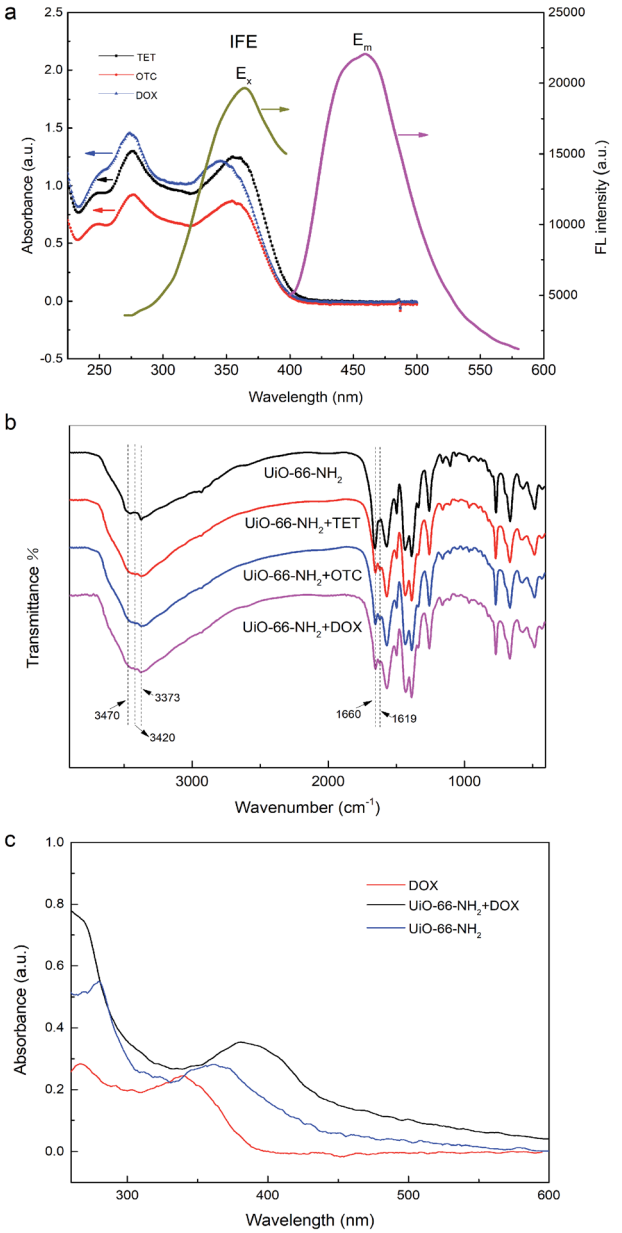

Fig. 7 (a) The UV spectra of TCs, and fluorescence spectra of UiO-66-NH_2 (E_x, fluorescence excitation spectrum of UiO-66-NH_2; E_m, fluorescence emission spectrum of UiO-66-NH_2). (b) The FT-IR spectra of UiO-66-NH_2 and UiO-66-NH_2 + TCs. (c) The UV spectra of DOX and UiO-66-NH_2 (in the presence and absence of DOX).

further indicated that a new complex was formed by the interaction between TCs and UiO-66-NH_2.[7] Thus, a driving force was generated for the electron transfer from –NH_2 on UiO-66-NH_2 to –CO–/–OH of TCs, explaining the fluorescence quenching phenomenon.[7,36,75,76] These results proved that IFE and PET were responsible for the luminescence quenching of UiO-66-NH_2.

3.6. Selectivity of UiO-66-NH_2 system

In the actual detection process, the possible coexisting substances in milk might affect the accuracy of the experimental results. Hence, to verify the selectivity of the established fluorescence sensing method, some other antibiotics (including chloramphenicol, amoxicillin and ampicillin), amino acids (tyrosine, serine, arginine, histidine, cysteine, and phenylalanine) and metal ions (Zn^{2+}, Al^{3+}, Mg^{2+}, Mn^{2+}, Ca^{2+}, K^+, and Na^+) were each added to the UiO-66-NH_2 system in the presence of TCs. As demonstrated in Fig. 8, compared with TCs (blank, 50 μM), the effects of these interfering substances on the fluorescence of UiO-66-NH_2 system were negligible, even if the concentrations of potential molecule and ion interfering substances were 5 times and 30 times higher than those of TCs, respectively. All the results illustrated that the UiO-66-NH_2 system had an excellent selectivity and a high specific recognition for the assay of TCs in complex matrix.

3.7. Precision detection of the developed fluorescence assay

The intra- and inter-day precision parameters were evaluated using the TCs standard solutions at three concentrations of 5, 20 and 40 μM. The results showed that the relative standard deviations (RSDs) ranged from 0.63% to 3.40% and from 0.75% to 3.29% ($n = 6$), respectively (Table S1†) (see ESI†). Therefore, this method has good accuracy and stability, which proves the feasibility of detecting TCs.

3.8. Analysis in practical samples

To further evaluate the practicability of UiO-66-NH_2 sensor in milk, spiking and recovery studies were carried out. No TCs were detected in milk samples purchased from local supermarkets (Fig. S4b†). A series of TCs standard solutions with different concentrations (0, 5, 20, 40 μM) were added to milk to obtain the blank and spiked samples. After pre-treatment, the above samples were analysed by the developed fluorescence sensing method, and the actual detection concentrations of the spiked samples were determined with the standard curves and regression equations. As clearly presented in Table S2,† the recoveries of TCs ranged from 93.26% to 115.17%, and the

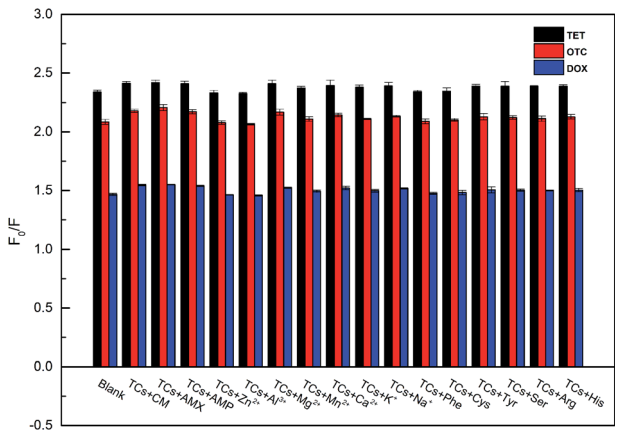

Fig. 8 Fluorescence responses of UiO-66-NH_2 to other antibiotics (5-fold concentration of TCs), amino acids (5-fold concentration of TCs), and ions (30-fold concentration of TCs) in the presence of TCs (50 μM).

Open Access Article. Published on 17 August 2022. Downloaded on 7/15/2025 3:50:19 PM. This article is licensed under a Creative Commons Attribution-NonCommercial 3.0 Unported Licence.

Table 1 A comparative table of different analytical approaches for the detection of TCs[a]

Method	Sample	Analyte	Linear range (μM)	LOD (μM)	Recovery (%)	Ref.
Fluorescent sensor of UiO-66-NH_2	Milk	TET/OTC/DOX	0–7.5/0–7.5/0–40	0.449/0.431/0.163	93.26–115.17	This study
Electrochemistry, based on MCPE	Urine/serum	DOX	0.1–10000/0.122–10000	0.10/0.12	98.1–99.37	77
Electrochemistry based on SbFE	Honey	TET	0.40–3.00	0.15	91.46–105.54	78
SERS	Duck meat	TET	9–56	2.52	101–108	9
Mesoporous fluorescent sensor based on ZnO NRs	Water	TET	2.0–120	1.27	102.37–103.51	79
Fluorescent probe based on SiQDs	Milk	OTC	2–20	0.43	98.8–100.5	80
Fluorescent sensor of Zn-MOF	Sea water	TET	1–75	0.234	98.3–102.3	81
Fluorescent sensor of NAC@Ag NCs	Milk	TET	1.12–230	0.47	98.2–102	19
Fluorescent probe of MRFNs	Water	TET	0.67–67	0.579	92.88–102	17
Fluorescent probe based CDs	Water/milk/pork	OTC	0–40	0.41	93.9–105	4
Ratiometric fluorescent sensor based on BNQD-Eu^{3+}	Milk/beef	TET/OTC/DOX	0–50	0.019/0.104/0.028	88.46–113.47	18
Ratiometric fluorescent probe of S dots/Ca^{2+}	Milk/fish	DOX	0.5–25	0.19	91–110	82
Fluorescent sensor based on CDs@MOF (Eu)	Simulated biological system	DOX	0–60	0.36	93.95–102.28	83

[a] MCPE: modified carbon paste electrode; SbFE: antimony film electrode; SERS: surface enhanced Raman spectroscopy; NRs: nanorods; SiQDs: silicon quantum dots; MOFs: metal–organic frameworks; NAC: *N*-acetyl-L-cysteine; Ag NCs: silver nanoclusters; MRFNs: Maillard reaction fluorescent nanoparticles; CDs: carbon dots; BNQD: boron nitride quantum dot; S dots: sulfur quantum dots and calcium ion.

relative standard deviations (RSDs, $n = 3$) were in the range of 0.50–2.92%. At the same time, the traditional high performance liquid chromatography (HPLC) method was applied to validate the reliability of the proposed fluorescence sensing method and the results were consistent with that determined by fluorescence assay (Table S2†).

As seen from the chromatogram in Fig. S4a,† the retention times of TET, OTC and DOX were 5.40, 6.58 and 26.28 min, respectively. There was a linear relationship between the HPLC method and fluorescence assay, which was shown in Fig. S5,† and the correlation coefficient (R^2) was 0.99483, illustrating that the accuracy of the proposed fluorescence method was equivalent to that of HPLC method. Therefore, above results indicated that the developed. UiO-66-NH_2 sensor was reliable and accurate to detect TCs in actual milk samples.

To our knowledge, there was no report on the detection of TCs in milk with UiO-66-NH_2 fluorescent sensor. The comparison between this method and existing approaches was presented in Table 1. It was found that the established assay in this paper had different advantages in linear detection range and detection limit. The linearity range of the proposed methodology was similar to that of surface-enhanced Raman spectroscopy (SERS) method, but the detection limit was relatively low. Furthermore, although the sensitivity of the proposed method was not as sensitive as electrochemical method, and the LOD and linear range were equivalent to many other fluorescence methods, the developed approach was easy and simple to operate. In view of the satisfactory recovery, low detection limit, wide linear range, and simplicity of operation, the established UiO-66-NH_2 sensing method could be applicable for TCs determination in practical samples.

4. Conclusions

In this study, a simple microwave-assisted synthesis method was used to fabricate a zirconium-based fluorescent metal–organic framework UiO-66-NH_2 sensor for the detection of TCs in milk. At the excitation wavelength of 365 nm, UiO-66-NH_2 has a strong and stable fluorescence emission intensity at the wavelength of 457 nm. Based on the PET (electron transfer from the ligand of UiO-66-NH_2 to –CO–/–OH on TCs) and IFE mechanisms, the fluorescence sensor showed rapid fluorescence quenching response (5 min) to target TCs, and exhibited a good selectivity and sensitivity with a linearity range of 0–47.5 μM and low detection limits (0.449 μM for TET, 0.431 μM for OTC, and 0.163 μM for DOX, lower than the maximum residue limit of 676 nM for TCs in milk defined by the FDA in US). Besides, the prepared UiO-66-NH_2 sensor was successfully utilized in the quantitative detection of TCs in milk samples, coupled with reasonable recoveries (93.26–115.17%) and low RSD values. The accuracy and reliability of UiO-66-NH_2 sensing assay were also verified by HPLC method. This paper may provide a new and promising approach for accurately, rapidly, sensitively, and selectively detecting TCs in complicated matrix samples.

Author contributions

All authors contributed to the study conception and design. Xiaohui Wang developed the idea of the study, presided over the design and coordination of the research, and completed the manuscript. Xufeng Wang contributed to the acquisition and interpretation of data. All authors provided critical review and

© 2022 The Author(s). Published by the Royal Society of Chemistry

Open Access Article. Published on 17 August 2022. Downloaded on 7/15/2025 3:50:19 PM. This article is licensed under a Creative Commons Attribution-NonCommercial 3.0 Unported Licence.

Xiaohui Wang substantially revised the manuscript. All authors read and approved the final manuscript.

Conflicts of interest

There are no conflicts to declare.

Acknowledgements

This work was supported by the Tianjin Research Innovation Project for Postgraduate Students (project no. 2019YJSB011).

Notes and references

1 I. Chopra and M. Roberts, *Microbiol. Mol. Biol. Rev.*, 2001, **65**, 232.
2 A. K. Sarmah, M. T. Meyer and A. B. A. Boxall, *Chemosphere*, 2006, **65**, 725–759.
3 N. Kemper, *Ecol. Indic.*, 2008, **8**, 1–13.
4 Y. Z. Fu, L. Huang, S. J. Zhao, X. J. Xing, M. H. Lan and X. Z. Song, *Spectroc. Acta Pt. A-Molec. Biomolec. Spectr.*, 2021, **246**, 6.
5 X. G. Hu, Q. X. Zhou and Y. Luo, *Environ. Pollut.*, 2010, **158**, 2992–2998.
6 L. L. Ji, W. Chen, L. Duan and D. Q. Zhu, *Environ. Sci. Technol.*, 2009, **43**, 2322–2327.
7 C. H. Li, L. Zhu, W. X. Yang, X. He, S. L. Zhao, X. S. Zhang, W. Z. Tang, J. L. Wang, T. L. Yue and Z. H. Li, *J. Agric. Food Chem.*, 2019, **67**, 1277–1283.
8 F. Cetinkaya, A. Yibar, G. E. Soyutemiz, B. Okutan, A. Ozcan and M. Y. Karaca, *Food Addit. Contam., Part B*, 2012, **5**, 45–49.
9 J. H. Zhao, P. Liu, H. C. Yuan, Y. J. Peng, Q. Hong and M. H. Liu, *J. Spectrosc.*, 2016, **2016**, 6.
10 J. Song, Z. H. Zhang, Y. Q. Zhang, C. Feng, G. N. Wang and J. P. Wang, *Anal. Methods*, 2014, **6**, 6459–6466.
11 S. H. Abou-Raya, A. R. Shalaby, N. A. Salama, W. H. Emam and F. M. Mehaya, *J. Food Drug Anal.*, 2013, **21**, 80–86.
12 V. Gaudin, *Biosens. Bioelectron.*, 2017, **90**, 363–377.
13 B. M. Marshall and S. B. Levy, *Clin. Microbiol. Rev.*, 2011, **24**, 718–733.
14 A. Onal, *Food Chem.*, 2011, **127**, 197–203.
15 R. Q. Fan, S. S. Tang, S. L. Luo, H. Liu, W. J. Zhang, C. J. Yang, L. D. He and Y. Q. Chen, *Molecules*, 2020, **25**, 12.
16 A. Khataee, R. Jalili, M. Dastborhan, A. Karimi and A. E. F. Azar, *Spectroc. Acta Pt. A-Molec. Biomolec. Spectr.*, 2020, **242**, 7.
17 X. J. Si, H. L. Wang, T. H. Wu and P. Wang, *RSC Adv.*, 2020, **10**, 43256–43261.
18 K. R. Yang, P. Jia, J. J. Hou, T. Bu, X. Y. Sun, Y. N. Liu and L. Wang, *ACS Sustainable Chem. Eng.*, 2020, **8**, 17185–17193.
19 Y. Zhang, M. Lv, P. F. Gao, G. M. Zhang, L. H. Shi, M. J. Yuan and S. M. Shuang, *Sens. Actuators, B*, 2021, **326**, 13.
20 A. Motorina, O. Tananaiko, I. Kozytska, V. Raks, R. Badia, M. E. Diaz-Garcia and V. N. Zaitsev, *Sens. Actuators, B*, 2014, **200**, 198–205.
21 L. Bovanova and E. Brandsteterova, *J. Chromatogr. A*, 2000, **880**, 149–168.
22 X. J. Lai, J. Liu, X. Xu, J. Li, B. J. Zhang, L. J. Wei, H. P. Cai and X. L. Cheng, *J. Sep. Sci.*, 2020, **43**, 398–405.
23 S. Lebedinets, C. Vakh, K. Cherkashina, A. Pochivalov, L. Moskvin and A. Bulatov, *J. Chromatogr. A*, 2020, **1615**, 8.
24 L. Wang, B. X. Yang, X. S. Zhang and H. G. Zheng, *Food Anal. Methods*, 2017, **10**, 2001–2010.
25 I. S. Ibarra, J. A. Rodriguez, J. M. Miranda, M. Vega and E. Barrado, *J. Chromatogr. A*, 2011, **1218**, 2196–2202.
26 G. F. Mu, H. T. Liu, L. N. Xu, L. H. Tian and F. Luan, *Food Anal. Methods*, 2012, **5**, 148–153.
27 J. Adrian, F. Fernandez, F. Sanchez-Baeza and M. P. Marco, *J. Agric. Food Chem.*, 2012, **60**, 3837–3846.
28 N. Pastor-Navarro, A. Maquieira and R. Puchades, *Anal. Bioanal. Chem.*, 2009, **395**, 907–920.
29 G. Wang, H. C. Zhang, J. Liu and J. P. Wang, *Anal. Biochem.*, 2019, **564**, 40–46.
30 H. Koike, M. Kanda, H. Hayashi, Y. Matsushima, T. Nakajima, S. Yoshikawa, Y. Ohba, M. Hayashi, C. Nagano, K. Sekimura, K. Otsuka, T. Hashimoto and T. Sasamoto, *Food Addit. Contam., Part B*, 2021, **14**, 66–73.
31 K. D. Pham, G. Degand, S. Danyi, G. Pierret, P. Delahaut, D. T. Vu, G. Maghuin-Rogister and M. L. Scippo, *Anal. Chim. Acta*, 2010, **672**, 30–39.
32 M. Kurzawa and A. Kowalczyk-Marzec, *J. Pharm. Biomed. Anal.*, 2004, **34**, 95–102.
33 A. Wong, M. Scontri, E. M. Materon, M. R. V. Lanza and M. Sotomayor, *J. Electroanal. Chem.*, 2015, **757**, 250–257.
34 Z. T. Wu, Y. B. Zhou, H. Y. Huang, Z. Su, S. M. Chen and M. C. Rong, *Sens. Actuators, B*, 2021, **332**, 8.
35 T. L. Wang, Q. S. Mei, Z. H. Tao, H. T. Wu, M. Y. Zhao, S. Wang and Y. Q. Liu, *Biosens. Bioelectron.*, 2020, **148**, 7.
36 Y. Q. Zhang, X. H. Wu, S. Mao, W. Q. Tao and Z. Li, *Talanta*, 2019, **204**, 344–352.
37 W. Y. Li, J. C. Zhu, G. C. Xie, Y. K. Ren and Y. Q. Zheng, *Anal. Chim. Acta*, 2018, **1022**, 131–137.
38 H. L. Tan and Y. Chen, *Sens. Actuators, B*, 2012, **173**, 262–267.
39 J. H. Guo, W. J. Lu, H. L. Zhang, Y. T. Meng, F. F. Du, S. M. Shuang and C. Dong, *Sens. Actuators, B*, 2021, **330**, 8.
40 Q. Ouyang, Y. Liu, Q. S. Chen, Z. M. Guo, J. W. Zhao, H. H. Li and W. W. Hu, *Food Control*, 2017, **81**, 156–163.
41 W. Wei, J. He, Y. Y. Wang and M. J. Kong, *Talanta*, 2019, **204**, 491–498.
42 P. Jia, T. Bu, X. Y. Sun, Y. N. Liu, J. H. Liu, Q. Z. Wang, Y. H. Shui, S. W. Guo and L. Wang, *Food Chem.*, 2019, **297**, 7.
43 Z. C. Hu, B. J. Deibert and J. Li, *Chem. Soc. Rev.*, 2014, **43**, 5815–5840.
44 W. P. Lustig, S. Mukherjee, N. D. Rudd, A. V. Desai, J. Li and S. K. Ghosh, *Chem. Soc. Rev.*, 2017, **46**, 3242–3285.
45 L. E. Kreno, K. Leong, O. K. Farha, M. Allendorf, R. P. Van Duyne and J. T. Hupp, *Chem. Rev.*, 2012, **112**, 1105–1125.
46 Y. J. Cui, Y. F. Yue, G. D. Qian and B. L. Chen, *Chem. Rev.*, 2012, **112**, 1126–1162.
47 Z. Yin, S. Wan, J. Yang, M. Kurmoo and M. H. Zeng, *Coord. Chem. Rev.*, 2019, **378**, 500–512.
48 Z. Ni and R. I. Masel, *J. Am. Chem. Soc.*, 2006, **128**, 12394–12395.

© 2022 The Author(s). Published by the Royal Society of Chemistry

Open Access Article. Published on 17 August 2022. Downloaded on 7/15/2025 3:50:19 PM. This article is licensed under a Creative Commons Attribution-NonCommercial 3.0 Unported Licence.

49 X. F. Wang, Y. B. Zhang, H. Huang, J. P. Zhang and X. M. Chen, *Cryst. Growth Des.*, 2008, **8**, 4559–4563.
50 S. Yuan, L. Feng, K. C. Wang, J. D. Pang, M. Bosch, C. Lollar, Y. J. Sun, J. S. Qin, X. Y. Yang, P. Zhang, Q. Wang, L. F. Zou, Y. M. Zhang, L. L. Zhang, Y. Fang, J. L. Li and H. C. Zhou, *Adv. Mater.*, 2018, **30**, 35.
51 Y. Bai, Y. B. Dou, L. H. Xie, W. Rutledge, J. R. Li and H. C. Zhou, *Chem. Soc. Rev.*, 2016, **45**, 2327–2367.
52 Y. N. Dou, L. Guo, G. L. Li, X. X. Lv, L. Xia and J. You, *Microchem. J.*, 2019, **146**, 366–373.
53 T. Lu, L. C. Zhang, M. X. Sun, D. Y. Deng, Y. Y. Su and Y. Lv, *Anal. Chem.*, 2016, **88**, 3413–3420.
54 Z. H. Xiang, C. Q. Fang, S. H. Leng and D. P. Cao, *J. Mater. Chem. A*, 2014, **2**, 7662–7665.
55 M. Kandiah, M. H. Nilsen, S. Usseglio, S. Jakobsen, U. Olsbye, M. Tilset, C. Larabi, E. A. Quadrelli, F. Bonino and K. P. Lillerud, *Chem. Mater.*, 2010, **22**, 6632–6640.
56 Y. F. Zhao, D. F. Wang, W. Wei, L. Z. Cui, C. W. Cho and G. P. Wu, *Environ. Sci. Pollut. Res.*, 2021, **28**, 7068–7075.
57 H. L. Zhu, J. P. Huang, Q. Y. Zhou, Z. W. Lv, C. Y. Li and G. Hu, *J. Lumin.*, 2019, **208**, 67–74.
58 C. Y. Sun, R. F. Su, J. X. Bie, H. J. Sun, S. N. Qiao, X. Y. Ma, R. Sun and T. H. Zhang, *Dyes Pigm.*, 2018, **149**, 867–875.
59 J. Xu, X. K. Shen, L. Jia, T. Zhou, T. L. Ma, Z. Q. Xu, J. L. Cao, Z. J. Ge, N. Bi, T. F. Zhu, S. L. Guo and X. H. Li, *J. Hazard. Mater.*, 2018, **342**, 158–165.
60 X. Fang, S. B. Wu, Y. H. Wu, W. Yang, Y. L. Li, J. Y. He, P. D. Hong, M. X. Nie, C. Xie, Z. J. Wu, K. S. Zhang, L. T. Kong and J. H. Liu, *Appl. Surf. Sci.*, 2020, **518**, 10.
61 L. Liu, W. Cui, C. Lu, A. B. Zain, W. Zhang, G. X. Shen, S. Q. Hu and X. Y. Qian, *J. Environ. Manage.*, 2020, **268**, 9.
62 C. M. Li, J. P. Huang, H. L. Zhu, L. L. Liu, Y. M. Feng, G. Hu and X. B. Yu, *Sens. Actuators, B*, 2017, **253**, 275–282.
63 K. Y. A. Lin, Y. T. Liu and S. Y. Chen, *J. Colloid Interface Sci.*, 2016, **461**, 79–87.
64 P. Karthik, A. Pandikumar, M. Preeyanghaa, M. Kowsalya and B. Neppolian, *Microchim. Acta*, 2017, **184**, 2265–2273.
65 Y. R. Du, X. Q. Li, H. J. Zheng, X. J. Lv and Q. Jia, *Anal. Chim. Acta*, 2018, **1001**, 134–142.
66 Z. Q. Yang, X. W. Tong, J. N. Feng, S. He, M. L. Fu, X. J. Niu, T. P. Zhang, H. Liang, A. Ding and X. C. Feng, *Chemosphere*, 2019, **220**, 98–106.
67 Y. Pan, X. Z. Yuan, L. B. Jiang, H. Wang, H. B. Yu and J. Zhang, *Chem. Eng. J.*, 2020, **384**, 16.
68 X. Y. He, F. Deng, T. T. Shen, L. M. Yang, D. Z. Chen, J. F. Luo, X. B. Luo, X. Y. Min and F. Wang, *J. Colloid Interface Sci.*, 2019, **539**, 223–234.
69 S. Chen, Y. L. Yu and J. H. Wang, *Anal. Chim. Acta*, 2018, **999**, 13–26.
70 Y. Zhou, Q. Yang, D. N. Zhang, N. Gan, Q. P. Li and J. Cuan, *Sens. Actuators, B*, 2018, **262**, 137–143.
71 G. W. Chen, F. L. Song, X. Q. Xiong and X. J. Peng, *Ind. Eng. Chem. Res.*, 2013, **52**, 11228–11245.
72 J. Y. Zhang, R. H. Zhou, D. D. Tang, X. D. Hou and P. Wu, *TrAC, Trends Anal. Chem.*, 2019, **110**, 183–190.
73 L. Han, Y. Z. Fan, M. Qing, S. G. Liu, Y. Z. Yang, N. B. Li and H. Q. Luo, *ACS Appl. Mater. Interfaces*, 2020, **12**, 47099–47107.
74 H. L. Tan, X. Y. Wu, Y. H. Weng, Y. J. Lu and Z. Z. Huang, *Anal. Chem.*, 2020, **92**, 3447–3454.
75 L. Zhang and L. Chen, *ACS Appl. Mater. Interfaces*, 2016, **8**, 16248–16256.
76 L. Chen, D. H. Liu, L. M. Zheng, S. M. Yi and H. He, *Anal. Bioanal. Chem.*, 2021, **413**, 4227–4236.
77 T. A. Ali, G. G. Mohamed, A. Z. El-Sonbati, M. A. Diab and A. M. Elkfass, *Russ. J. Electrochem.*, 2018, **54**, 1081–1095.
78 G. Krepper, G. D. Pierini, M. F. Pistonesi and M. S. Di Nezio, *Sens. Actuators, B*, 2017, **241**, 560–566.
79 Z. P. Zhou, K. Lu, X. Wei, T. F. Hao, Y. Q. Xu, X. D. Lv and Y. F. Zhang, *RSC Adv.*, 2016, **6**, 71061–71069.
80 H. E. Satana Kara, B. Demirhan and B. Er Demirhan, *Turk. J. Chem.*, 2020, **44**, 1713–1722.
81 B. Zhu, Z. Zong, X. Zhang, D. M. Zhang, L. S. Cui, C. F. Bi and Y. H. Fan, *Appl. Organomet. Chem.*, 2020, **34**, 11.
82 Y. R. Zhuang, B. X. Lin, Y. Yu, Y. M. Wang, L. Zhang, Y. J. Cao and M. L. Guo, *Food Chem.*, 2021, **356**, 8.
83 X. Fu, R. Lv, J. Su, H. Li, B. Y. Yang, W. Gu and X. Liu, *RSC Adv.*, 2018, **8**, 4766–4772.

© 2022 The Author(s). Published by the Royal Society of Chemistry